Vertical Air Motion from T-REX Radiosonde and Dropsonde Data

JUNHONG WANG

Earth Observing Laboratory, National Center for Atmospheric Research, Boulder, Colorado*

JIANCHUN BIAN

Laboratory for Middle Atmosphere and Global Environment Observation (LAGEO), Institute of Atmospheric Physics, Chinese Academy of Sciences, Beijing, China

WILLIAM O. BROWN AND HAROLD COLE

Earth Observing Laboratory, National Center for Atmospheric Research, Boulder, Colorado*

VANDA GRUBIŠIĆ

Desert Research Institute, Reno, Nevada

KATE YOUNG

Earth Observing Laboratory, National Center for Atmospheric Research, Boulder, Colorado*

(Manuscript received 6 October 2008, in final form 8 December 2008)

ABSTRACT

The primary goal of this study is to explore the potential for estimating the vertical velocity (VV) of air from the surface to the stratosphere, using widely available radiosonde and dropsonde data. The rise and fall rates of radiosondes and dropsondes, respectively, are a combination of the VV of the atmosphere and still-air rise–fall rates. The still-air rise–fall rates are calculated using basic fluid dynamics and characteristics of radiosonde and dropsonde systems. This study validates the technique to derive the VV from radiosonde and dropsonde data and demonstrates its value. This technique can be easily implemented by other users for various scientific applications.

The technique has been applied to the Terrain-induced Rotor Experiment (T-REX) dropsonde and radiosonde data. Comparisons among radiosonde, dropsonde, aircraft, and profiling radar vertical velocities show that the sonde-estimated VV is able to capture and describe events with strong vertical motions (larger than ~1 m s^{-1}) observed during T-REX. The VV below ~5 km above ground, however, is overestimated by the radiosonde data. The analysis of derived VVs shows interesting features of gravity waves, rotors, and turbulence. Periodic variations of vertical velocity in the stratosphere, as indicated by the radiosonde data, correspond to the horizontal wavelength of gravity waves with an averaged horizontal wavelength of ~15 km. Two-dimensional VV structure is described in detail by successive dropsonde deployment.

1. Introduction

The vertical motion of the atmosphere represents atmospheric dynamics ranging from small-scale turbulence in the planetary boundary layer (PBL) and inside clouds to various types of waves and the large-scale ascending and descending parts of meridional circulations. The measurement of vertical velocity (VV) in PBL is important for calculating air–surface transport of mass and energy. Vertical motion inside clouds affects cloud formation (e.g., Paluch and Lenschow 1991) and the partitioning of water phases within clouds (e.g., Rauber and Tokay 1991). The vertical velocity is required to characterize gravity waves and their propagation, evolution and dissipation, and parameterization in numerical

* The National Center for Atmospheric Research is sponsored by the National Science Foundation.

Corresponding author address: Junhong Wang, NCAR/EOL, P.O. Box 3000, Boulder, CO 80307.
E-mail: junhong@ucar.edu

DOI: 10.1175/2008JTECHA1240.1

models (Kim et al. 2003). Mean vertical motion in the tropical atmosphere provides a good depiction of vertical circulation within the convective and stratiform portion of the tropical mesoscale convective complex (e.g., Balsley et al. 1988; Gage et al. 1991).

In view of the importance of vertical motion in the atmosphere, it is crucial to measure the VV on all temporal and spatial scales. However, the VV is difficult to measure mainly because of its small magnitude (an order of a few centimeters per second; Holton 1992). In the past, the VV was not measured directly; instead it was derived from horizontal winds using the continuity equation. Over the past few decades, various techniques have been developed to directly measure the VV, including sonic anemometry on flux towers, airborne sensors, and ground-based remote sensors (radar, lidar, sodar, and wind profiler; e.g., Balsley et al. 1988; Van Zandt 2000; Contini et al. 2004; Shupe et al. 2008). Each of these instruments and techniques has its own strengths and limitations, and they all are expensive. The tower and airborne sensors are limited in vertical coverage, and the VV obtained from wind profilers is susceptible to several types of biases (Rao et al. 2008). The intent of this paper is to explore the potential to estimate the VV from the surface to the stratosphere using radiosonde and dropsonde data under all weather conditions.

The radiosonde balloon ascent rate and the dropsonde fall rate can be calculated from the pressure tendency if high-resolution radiosonde data are available or directly measured by the GPS receiver in GPS sondes. The ascent rate has been used to study atmospheric waves (e.g., Corby 1957; Reid 1972; Lalas and Einaudi 1980; Shutts et al. 1988; McHugh et al. 2008) and to estimate the boundary layer height (Johansson and Bergström 2005), and it is potentially a good indirect measure of turbulence (Johansson and Bergström 2005). McHugh et al. (2008) provide a thorough summary of previous studies of waves in the atmosphere using the radiosonde ascent rate. The dropsonde fall rate is much smoother than the radiosonde ascent rate because of the radiosonde's pendulum effect and self-induced balloon motion (MacCready 1965). The vertical velocity of the air has been computed from the dropsonde fall rate to study hurricane structures (Hock and Franklin 1999; Franklin et al. 2003; Stern and Aberson 2006).

In this study, we take advantage of over 400 high-resolution (1 s for radiosonde and 0.5 s for dropsonde) soundings collected during the Terrain-induced Rotor Experiment (T-REX) over Owens Valley, California, from March to April 2006. The technique to estimate the VV from the sonde data is refined for the T-REX data and described in detail. The technique is applied to the T-REX sounding data to produce a carefully quality-controlled VV-sounding dataset. The VV data are judged against other collocated aircraft and in situ data and are utilized to study several types of atmospheric phenomena with strong vertical motions sampled during T-REX.

The methods for estimating the VV from the T-REX data are presented in section 2. The methods are validated in section 3. The scientific highlights of sounding-derived VV data are provided in section 4. Section 5 summarizes the results and includes some remarks on the methods' limitations and future potential improvements.

2. Methods and data

a. Methods

The radiosonde rise and dropsonde fall rates can be directly measured by GPS receivers in the sonde or calculated from pressure tendency. The comparisons of measured and calculated rise–fall rates show very good agreement with a mean difference less than 0.1 m s^{-1} and an rms difference of 0.64 and 0.92 m s^{-1} for T-REX radiosonde and dropsonde data, respectively. We choose to work with the calculated rise–fall rates rather than those measured by the GPS because the GPS data often contain more missing points than pressure–temperature–humidity (PTU) data as a result of poor reception of GPS satellite signals. For T-REX, the percentage of missing data averaged for all soundings is 7% for PTU but 10% (23%) for GPS for radiosonde (dropsonde). The actual rise–fall rate is a combination of the VV of the ambient air and the ''still air'' rise–fall rate. The latter can be computed based on fluid dynamics and characteristics of radiosonde and dropsonde systems (see below). The VV is estimated by subtracting the still-air rise–fall rate from that in the actual atmosphere.

The radiosonde rise rate in the still air is calculated based on the balance of the buoyancy and drag force exerted on the sonde (e.g., Johansson and Bergström 2005). The buoyancy force (BF) is the difference between the free lifting and the total weight of the package and expressed as

$$\mathrm{BF} = \mathrm{BV}\rho g - (m_s + m_b + m_h)g, \tag{1}$$

where BV (m^3) is the balloon volume; ρ (kg m^{-3}) is the air density; g (m s^{-2}) is the acceleration due to gravity at the surface of earth; and m_s, m_b, and m_h are the weight (kg) of the radiosonde, balloon, and helium, respectively. The BV changes with height and equals to $\mathrm{BV}_0\rho_s/\rho$, where BV_0 is the balloon volume on the ground and ρ_s is the surface air density. BV_0 is not measured accurately: it is roughly estimated by the operator's eyes and varies from ~0.708 m^3 (25 ft^3) to ~0.991 m^3 (35 ft^3). For the

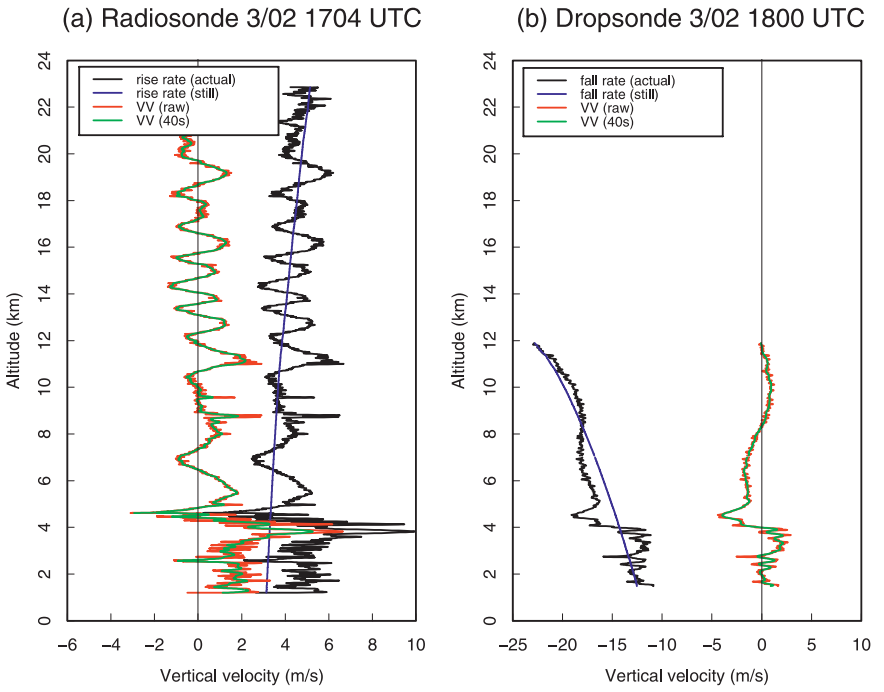

FIG. 1. The rise rate (m s^{-1}) in the actual and still air and the estimated unfiltered and filtered VV (m s^{-1}) for one (a) radiosonde and (b) dropsonde sounding each on 2 Mar 2006. The thin vertical black line denotes the 0 m s^{-1} line.

National Center for Atmospheric Research (NCAR) GPS Advanced Upper-Air Sounding System (GAUS) deployed in T-REX, m_s and m_b are equal to 295 and 200 g, respectively; and m_h is equal to $(4.0026\mathrm{BV}_0\rho_s)/28.9644$. The drag force (DF) is defined as

$$\mathrm{DF} = (C_{\mathrm{dr}}A_r\rho W_r^2)/2, \tag{2}$$

where C_{dr} is the drag coefficient of the balloon, A_r is the cross area of the balloon equal to $\pi[3\mathrm{BV}/(4\pi)]^{2/3}$, and W_r is the sonde rise rate in still air. From Eqs. (1) and (2), W_r is derived:

$$W_r = [2\mathrm{BF}/(C_{\mathrm{dr}}A_r\rho)]^{1/2}. \tag{3}$$

The drag coefficient of spheres (C_{dr}) depends on the Reynolds number (Re), which experiences a transition from supercritical value (~ 2–3×10^5) in the boundary layer or turbulent layer to subcritical value (~ 0.5–2×10^5) in the free troposphere (Vennard 1955; MacCready 1965). Consequently, C_{dr} can change from ~0.2 for supercritical conditions to ~0.5 for subcritical conditions (Vennard 1955). In addition, other factors, such as free stream turbulence and unsteadiness and nonspherical shape of the balloon during flight, also affect the value of C_{dr} (Lalas and Einaudi 1980).

The challenge to accurately calculate W_r from Eq. (3) lies in the uncertainty of BV_0 and C_{dr} discussed above. The sonde rise rate W_r is very sensitive to BV_0 and can increase from ~1.5 to ~4 m s^{-1} as BV_0 changes from 0.566 m^3 (20 ft^3) to 1.133 m^3 (40 ft^3). A striking feature of the balloon rise rate found in the soundings launched near Independence, California, during T-REX is that the rise rate below ~5 km MSL (the top of the mountain ridge) is larger and noisier (see, e.g., Fig. 1a). This is most likely a result of turbulence (Johansson and Bergström 2005). Turbulence lowers the critical Re and in turn decreases the drag coefficient resulting an increase in the rise rate. The smaller critical Re also makes the balloon operate at supercritical value, which generates the largest self-induced irregular balloon motions and then causes the larger variability. Therefore, it is difficult to estimate C_{dr} below 5 km.

The profile of Re for each sounding was calculated. Mean Re profile averaged for all soundings shows a transition from above 2.5×10^5 below about 5 km to less than 2×10^5 above 5 km, which corresponds well with the transition from the turbulent flow below 5 km to the laminar flow above. Based on Fig. 184 in Vennard (1955), it suggests a change of C_{dr} from ~0.2 below 5 km to ~0.4–0.5 above 5 km. However, the altitude where the transition occurs changes from one sounding to another and Re varies significantly below ~5 km. In addition, C_{dr} can change from 0.1 to 0.4 in the transitional regime. Therefore, it is challenging to use a uniform C_{dr} below a fixed altitude for all soundings.

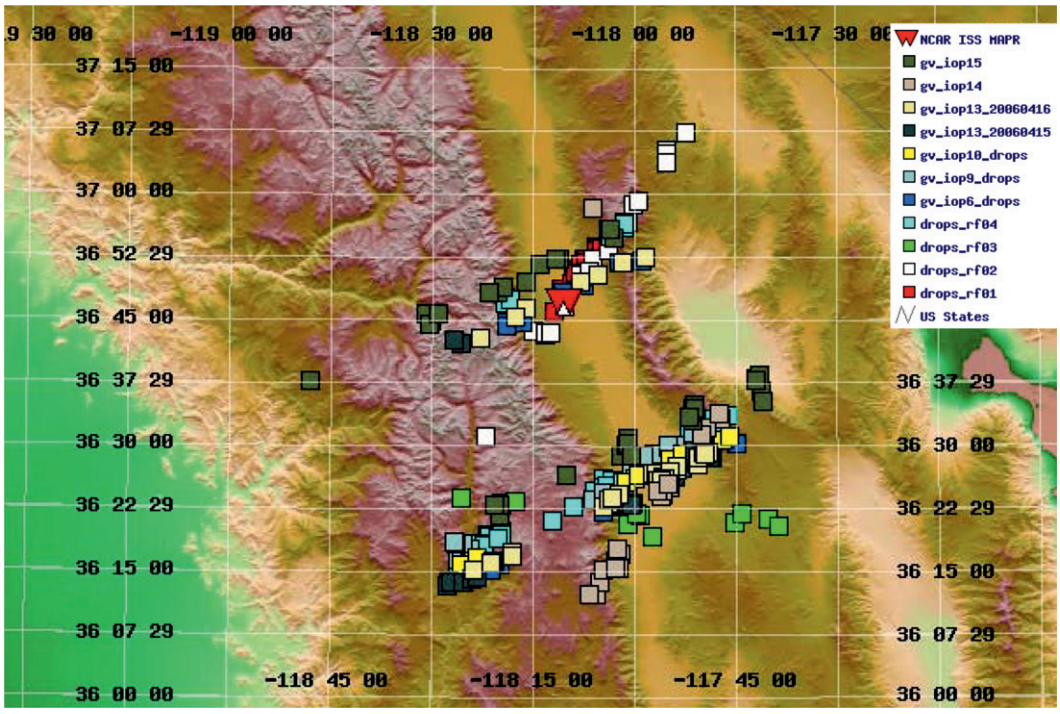

FIG. 2. Topographic map with launch locations of dropsondes (squares) and radiosondes [NCAR Integrated Sounding System (ISS) MAPR] during T-REX.

In this study, we vary BV_0 from ~0.708 m^3 (25 ft^3) to ~0.991 m^3 (35 ft^3) and C_{dr} from 0.4 to 0.5 to find optimal BV_0 and C_{dr} values for each sounding. For each pair of BV_0 and C_{dr} the median of VVs above 5 km is calculated. Then the pair that provides the minimum of median values is selected for that sounding. This is based on the assumption that VVs above 5 km have a normal distribution with a near-zero median value. The minimum of median values for 102 soundings ranges from 0 to 0.93 m s^{-1} with a mean of 0.02 m s^{-1}. In this way, C_{dr} is too large for the turbulent layer below 5 km where the flow has a supercritical Re. As a result, W_r is underestimated and, consequently, VV is overestimated below 5 km. The VV below 5 km represents a combination of environmental vertical velocity and abnormal rise rate caused by turbulence and other factors. Figure 1a shows one example of calculated rise rate in the actual and still air, derived VV, and smoothed VV. A 40-s low-pass filter is applied to the VV data to remove the noise from the pendulum effect, self-induced balloon motions, and other potential causes, such as the gas leakage and nonspherical shape of the balloon and turbulence.

The dropsonde fall rate in the still air W_d is computed based on the balance between the gravity [the left side of Eq. (4)] and the drag force [the right side of Eq. (4)] (Hock and Franklin 1999):

$$m_{sd}g = C_{dd}A_d\rho W_d^2/2, \quad (4)$$

where m_{sd} is the weight of the dropsonde (350 g), C_{dd} is the drag coefficient (0.61 for dropsonde), and A_d is the area of the parachute. The NCAR dropsonde uses a standard square parachute of 26 cm × 26 cm or a large one (50 cm × 50 cm). From Eq. (4) W_d is derived as

$$W_d = [2m_{sd}g/(C_{dd}A_d\rho)]^{1/2}. \quad (5)$$

An example is given in Fig. 1b. The dropsonde fall rate W_d decreases from ~23 m s^{-1} at 12 km to ~12 m s^{-1} near the ground. A 20-s low-pass filter is applied to the calculated W_d from Eq. (5) to remove occasional spikes in W_d.

b. Data

T-REX was conducted during March and April of 2006 in Owens Valley to explore the structure and evolution of atmospheric rotors, intense low-level turbulence zones that typically form parallel to and downstream from mountain ridge crests in close association with mountain waves (Grubišić et al. 2008). Many in situ and airborne instruments were deployed in T-REX to capture the vertical structure of the atmosphere in the valley. Among these instruments were NCAR GAUS and dropsonde systems. GAUS launches Vaisala RS92 radiosonde and provides vertical profiles of pressure, temperature, humidity,

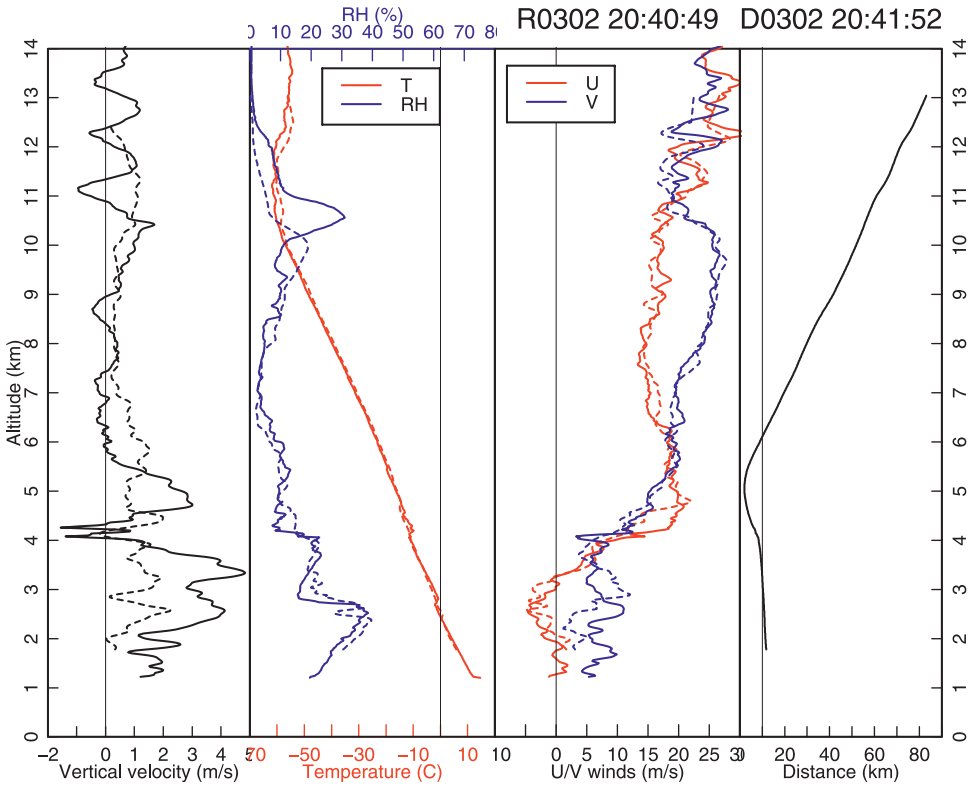

FIG. 3. Comparisons of profiles of VV (m s^{-1}), temperature (°C), RH (%), and zonal and meridional wind speeds (U/V; m s^{-1}) for radiosonde (solid line) and dropsonde (dashed line) launched at ~2041 UTC 2 Mar 2006, and distance (km; far right) between the radiosonde and dropsonde locations.

horizontal wind speed and direction, and balloon rise rate and position in a 1-s vertical resolution (~5 m). During T-REX, GAUS was located near Independence in Owens Valley (Fig. 2) and launched 102 radiosondes during the 2-month period. These soundings were collected to obtain kinematic and thermodynamic data for the valley atmosphere and, in conjunction with NCAR Mobile GAUS (MGAUS) soundings launched from the sites upwind of the Sierra Nevada, to detect changes induced on the lee side by mountain waves and rotors. Note that only GAUS data collected in Owens Valley are used in this study although we also processed the MGAUS data. The NCAR GPS dropsonde was developed in 1995 and is currently manufactured by Vaisala as Vaisala dropsonde RD93 (Hock and Franklin 1999; Vaisala 2004; Wang 2005). During T-REX, 306 dropsondes were deployed from the NCAR Gulfstream V (GV) aircraft during 11 research flights over Owens Valley and the surrounding mountain ranges (Fig. 2). The dropsonde data has 0.5 s vertical resolution, corresponding to ~5–10 m.

All T-REX radiosonde and dropsonde data have been carefully quality controlled using several methods including applying automatic sounding quality-control software called Atmospheric Sounding Processing Environment (ASPEN), visually examining each sounding for "reasonableness" based on the skew T–log$p$ and plotting the histogram and time series of each parameter. The methods for calculating the VV described in section 2a [Eqs. (3) and (5)] were applied to the T-REX radiosonde and dropsonde data to create a T-REX vertical velocity sounding dataset. In the dataset, both unsmoothed and smoothed VV are included. For the dropsonde data, 18 soundings were classified as "fast fall." This occurs when the parachute fails to deploy, resulting in the dropsonde falling at approximately twice the normal speed. Therefore, Eq. (5) is not suitable for the fast-fall soundings, and the 18 soundings were removed from the final dataset.

The 1-s air vertical velocity data from the University of Wyoming King Air collected during T-REX have an accuracy of 0.15 m s^{-1} for the whole flight (usually about or less than 4 h) and are used to validate VVs estimated from radiosonde and dropsonde data in section 3. Given the aircraft speed of about 100–120 m s^{-1}, a 1-s data sampling represents an average over 100–120 m. NCAR's Multiple Antenna Profiler (MAPR) was deployed near Independence, collocated with GAUS and

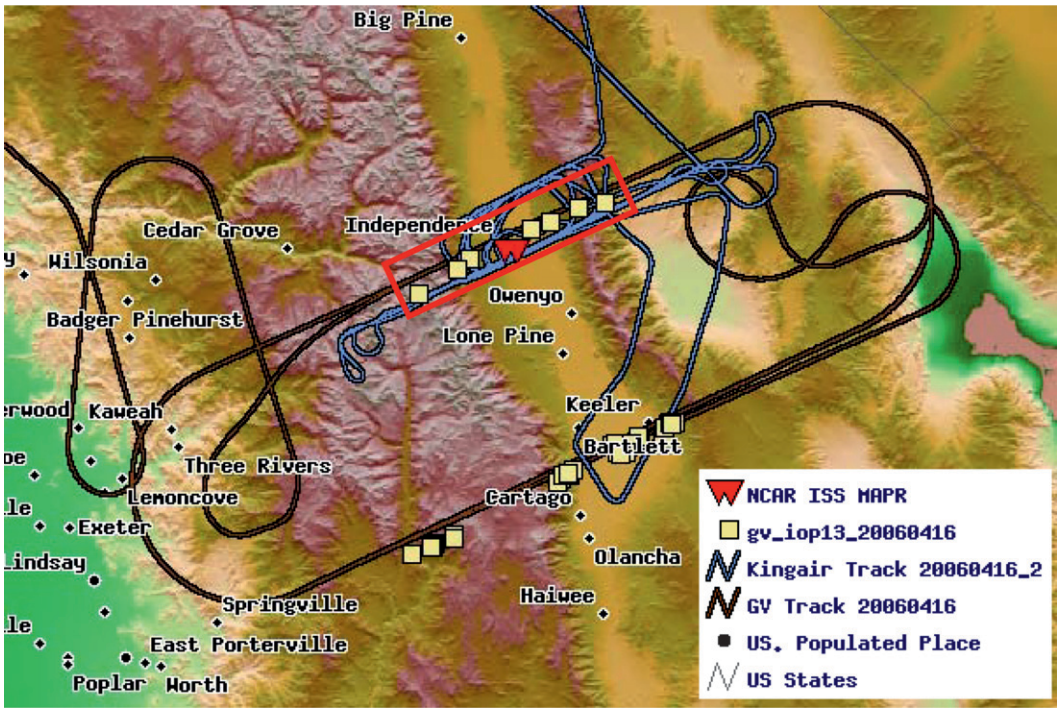

FIG. 4. King Air (blue) and GV (brown) flight tracks, dropsonde release locations (yellow squares), and the radiosonde site (NCAR ISS MAPR) during T-REX IOP 13.

provides continuous measurements of vertical velocity with an accuracy of ~0.3 m s^{-1} and a vertical resolution of 100 m in altitude. The estimated VV from GAUS data is matched and compared with the MAPR data.

3. Validation

It is difficult to validate the estimated VV from sounding data owing to the lack of coincident VV data from other measurements and large variability of the VV, both temporally and spatially. The VV changes from very small turbulent motion (an order of 0.1 cm s^{-1}) to strong updrafts of ~15 m s^{-1} in hurricane rainbands (Stern and Aberson 2006). In this section, we focus on comparing VV variations between radiosonde and dropsonde data, between sounding (both radiosonde and dropsonde) and aircraft, and between radiosonde and MAPR data to qualitatively assess the strength and limitation of the method.

Based on the discussions in section 2a, the method of estimating the VV from dropsonde data is superior to the one used for radiosondes because of the uncertainty in the balloon volume and drag coefficient for the radiosonde and no pendulum effects and self-induced motions for the dropsonde. The dropsonde parachute was carefully designed to provide accurate wind measurements by reducing rotation of the parachute and eliminating the pendulum motion of the dropsonde. The dropsonde drag coefficient (C_{dd}) was derived from wind tunnel measurements, verified against a theoretical model, and found to remain constant during the flight. Thus, good agreement between the VV derived from radiosonde and dropsonde data would give us confidence in the methods used. The dropsondes were selected for the following analysis if they were dropped within one-half hour of the radiosonde launch time. In addition, to ensure sufficient spatial overlap, the horizontal distance between radiosonde and dropsonde had to be less than 10 km within a layer of more than 3 km in depth. We found seven such matched soundings. It should be noted that on average the radiosonde horizontal drift is about 67 km as it rises from the ground to 12 km, whereas the dropsonde drifts on average 15 km as it descends from 12 km to the ground. Figure 3 shows comparisons of temperature, humidity, and horizontal and vertical wind profiles for one pair of soundings on 2 March in which the dropsonde was dropped within 2 min of the radiosonde launch time. The sondes were separated by less than 10 km below ~6.5 km, and then were separated by as much as 80 km at the altitude of 13 km. Temperature (T), relative humidity (RH), and horizontal wind show very good agreement between the radiosonde and dropsonde even above 6.5 km (Fig. 3). The small horizontal separation and similar structures

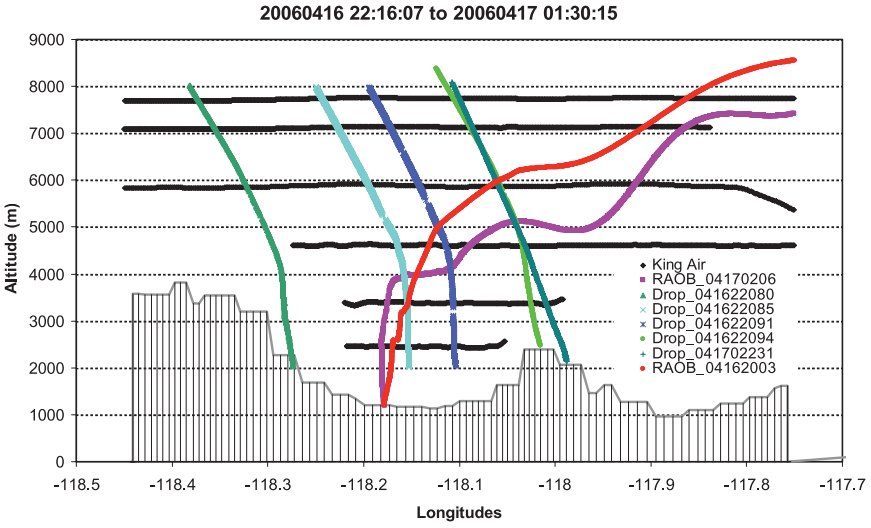

FIG. 5. King Air tracks (black dots), radiosonde (''RAOB''), and dropsonde (''Drop'') during the latter part of T-REX IOP 13 in a longitude–altitude plane. The date and UTC time are shown in the legend. The underlying terrain along the northern leg in Fig. 4 is marked by vertical gray lines. For the radiosondes, only tracks below 9 km and west of 117.75°W are plotted.

in *T*, RH, and wind suggest that the radiosonde and dropsonde sampled the same air mass. However, the VV profiles from the radiosonde and dropsonde are not comparable, and the radiosonde-estimated VV has a much larger magnitude than that from the dropsonde below 5 km. This suggests that the radiosonde method overestimates VV below 5 km because of the larger drag coefficient used, as discussed in section 2a. The waves in the 10–12-km range evident in the radiosonde VV data are absent in the dropsonde data. The absence of data may be because, at this altitude, the radiosonde is primarily sampling horizontal variations due to the waves, as will be shown in section 4. However, the dropsonde and radiosonde horizontal wind data show similar wave structures above 11 km. The other six sounding pairs show features similar to those shown in Fig. 3.

The intensive observing period (IOP) 13 during T-REX started at 2000 UTC 16 April and ended at 0800 UTC 17 April. Note that there is a 7-h difference

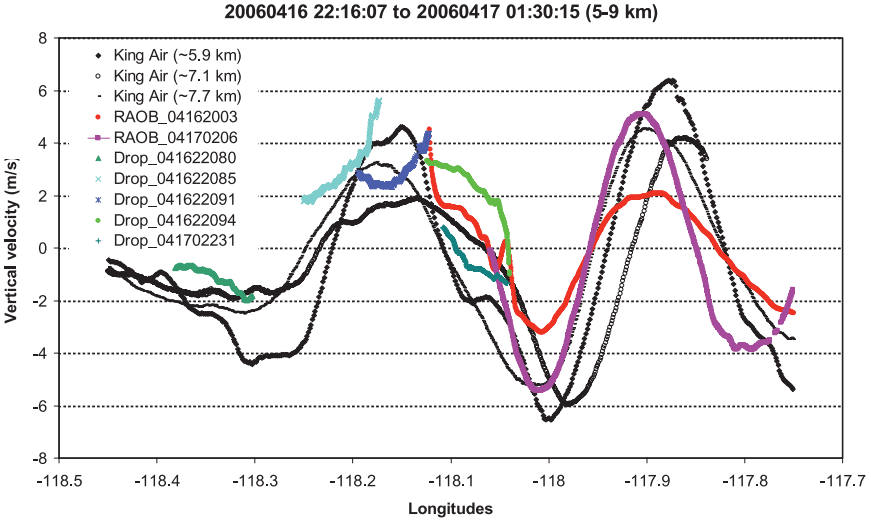

FIG. 6. Variations of VV with longitude from the King Air data at three altitudes, two radiosondes, and five dropsondes during T-REX IOP 13. The sounding data are only shown for the layer of 5–9 km and west of 117.75°W.

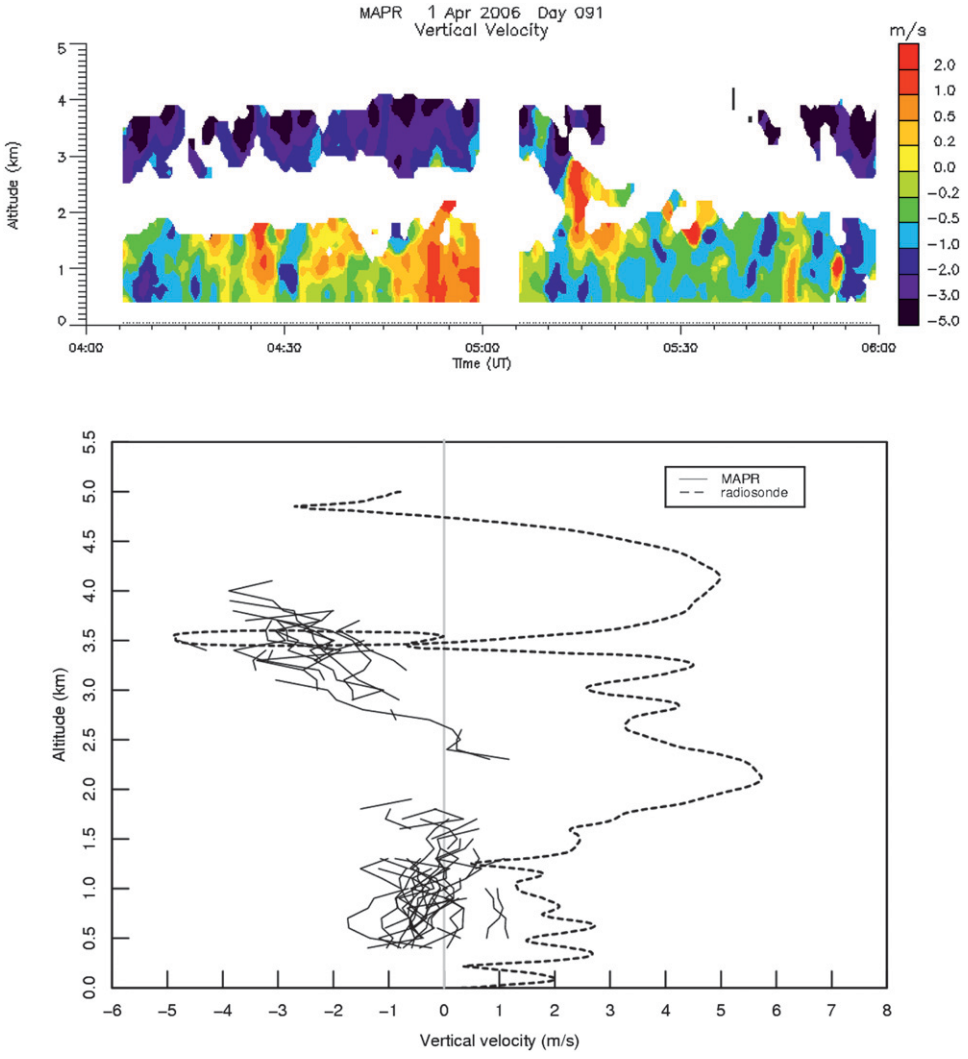

FIG. 7. The time series of MAPR VV profiles (top) from 0400 to 0600 UTC 1 Apr 2006 and the VV profile (bottom) from the sounding launched at 0459 UTC (dashed, black) along with the MAPR profiles (solid, black) 1 h before and after the sonde launch.

between UTC and Pacific standard time in the T-REX region. The IOP 13 was aimed at studying the coupled mountain-wave–rotor–boundary layer system. Figure 4 displays the tracks of the University of Wyoming King Air and NCAR GV aircrafts and the locations of radiosondes and dropsondes. Over the northern leg, NCAR GV dropped seven dropsondes, the King Air flew at different altitudes to sample both horizontal and vertical structures of the atmosphere, and two radiosondes were launched from Independence (Fig. 4). During the period from 2216 UTC 16 April to 0130 UTC 17 April, the King Air flew at six altitudes between 2 and 8 km above sea level (ASL) over Owens Valley where five dropsondes and two radiosondes were released (Fig. 5). The significant horizontal drift of radiosondes above 4 km is evident in Fig. 5. The VV data in the 5–9-km layer from the King Air and soundings are shown as a function of longitude in Fig. 6. The King Air data at three altitudes show similar waves with a wavelength of ~25 km, suggesting that the waves are stationary and have nearly vertical phase lines. Two radiosonde soundings nicely capture the wave structure east of Independence because of their large horizontal drift, indicating that the radiosonde data are representative of horizontal wave structures rather than vertical ones (for a more detailed discussion, see section 4). Dropsondes only sample a small portion of the wave because of their smaller horizontal drift, but a rapid sequence of consecutive dropsondes is able to capture the horizontal wave structure as well.

The radiosondes in Owens Valley were launched from the site where the MAPR provided high-resolution VV data. Nevertheless, it is very challenging to compare the VV profiles from the radiosondes and MAPR because of the large temporal variability of the VV (see Fig. 7, top panel), the quick drift of the radiosonde out of MAPR's range, and the fact that the MAPR data are only available within 5 km above ground level, where radiosonde-estimated VV bears the largest degree of uncertainty. Nevertheless, five soundings showing large vertical motions below 5 km were selected to compare with MAPR data. Figure 7 shows one example and is representative of all of the MAPR–sounding comparisons. The time series of MAPR data shows strong fluctuations of the VVs below 2 km and consistent downdrafts between ~2.5 and 4 km. The missing MAPR data in the range of ~1.5–2.5 km results from the very dry air there. The MAPR profiles 1 h before and after the sonde launch time are compared with the radiosonde profile. The sonde encountered a strong downdraft (>4 m s^{-1}) at ~3.5 km that forced the balloon downward ~100 m, which is consistent with what was seen in the MAPR data. The sonde drifted 5.17 km northeast of the MAPR site when it encountered the strong downdraft, indicating that the downdraft was a larger-scale feature. It is also evident from Fig. 7 that the VV estimated from the radiosonde data shows an updraft of ~2 m s^{-1} below 2 km, while the majority of MAPR profiles show a small downdraft there.

The techniques to estimate the VV from the radiosonde and dropsonde data work best with strong vertical motions because of uncertainties in calculated fall–rise rates in the real atmosphere and still air and other factors unaccounted for, such as the gas leakage from the balloon during the flight, the nonspherical shape of the balloon, and the balloon self-induced motions. Hence, it would be very useful to provide the users with the VV threshold at which the presented methods are useful. The mean and standard deviation of the VV from all 102 radiosonde profiles are shown in Fig. 8. Given a similarity of large-scale conditions during T-REX IOPs, radiosondes in general have similar trajectories, characterized by the advection to the northeast after their launches. Therefore, the mean profile is meaningful as the majority of sondes sampled the same segment of the atmosphere under similar weather conditions. The mean profile in Fig. 8 represents mean conditions along the balloon path and systematic errors in the estimated VV, whereas the standard deviation is a result of uncertainties in the method and temporal variability of the VV. As discussed before, the large values of the mean and standard deviation below 5 km are partially due to the overestimation of the radiosonde-derived VV. Above 5 km, one can see mean vertical motion of less than 0.5 m s^{-1} and the standard deviation of ~0.5–1 m s^{-1} with a mean of 0.86 m s^{-1}. This suggests that the maximum uncertainty in radiosonde-estimated VV above 5 km is 0.86 m s^{-1}. The same technique cannot be applied to the dropsonde data since dropsondes cover a large geographic area and hence show larger mean and standard deviation values (not shown). However, the VV threshold for the dropsonde is expected to be smaller than that for the radiosonde.

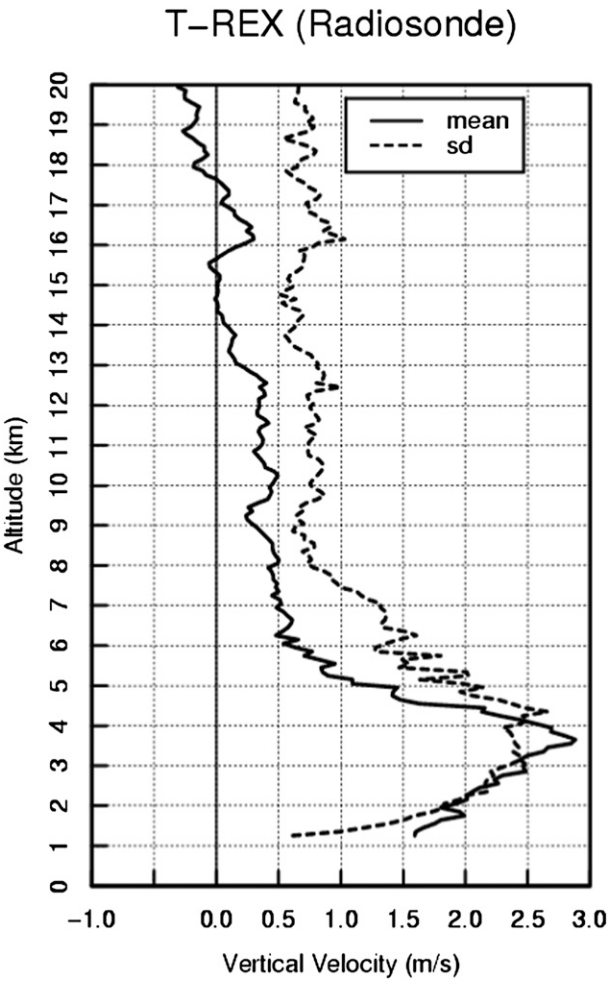

FIG. 8. Mean (solid) and standard deviation (dashed) of VV (m s^{-1}) for all 102 radiosonde profiles.

4. Scientific highlights

The VV profiles from radiosonde soundings launched in Owens Valley, as illustrated by the first 30 profiles during April 2006 in Fig. 9, are characterized by three features: 1) large magnitude and variability below the mountain ridge (~5 km), indicating the strong turbulence (see discussion in section 2); 2) frequent occurrence

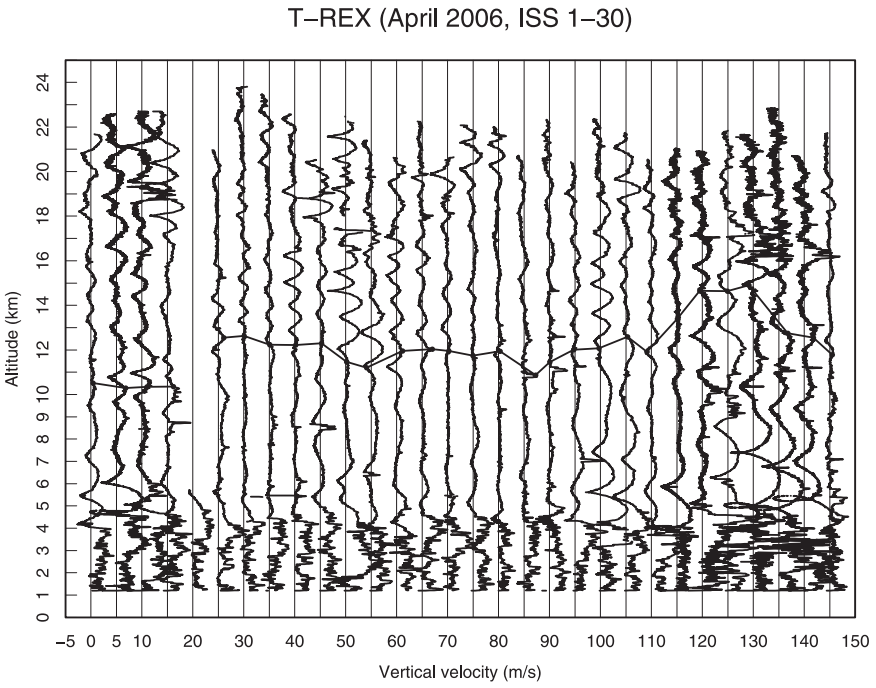

FIG. 9. Thirty unfiltered VV profiles (m s^{-1}) from soundings launched during April. The horizontal black lines denote tropopause heights. A 5 m s^{-1} offset is added for each sounding after the first one. For example, 145 m s^{-1} means 0 m s^{-1} for the 30th sounding.

of waves in the stratosphere; and 3) downdrafts seen in some of the soundings stronger than the balloon rise rate, causing the balloons to descend for a short period of time before ascending again. The last type of sounding is referred as to the ''loop'' sounding. Since it is not known how the turbulence affects the critical Re and therefore the rise rate, the feature below ~5 km is only an indication of turbulence existence and cannot be used to derive turbulence parameters. Results of the quantitative study of stratospheric waves and the loop soundings are presented below.

Of the 102 GAUS soundings, 12 were classified as loop soundings (Fig. 10). All loops, except one on 10 March, were located directly right above the low-level turbulent layer with VV ranging between −4.13 and −13.81 m s^{-1}. These loops are the result of sondes being caught in strong wave and/or rotor downdrafts. Figure 11 highlights the example from 0312 UTC 26 March. At ~5300 m MSL, this sonde was forced down approximately 1000 m by the environmental downdraft of 11.4 m s^{-1}. This strong downdraft was encountered by the sonde just upstream of the Inyo Mountains, which compose the eastern wall of Owens Valley. This strong downdraft is found at the interface between the warm and dry air from aloft and the colder and more humid air within the valley, which is characterized by a strong temperature inversion and pronounced wind shear. It is consistent with the large VVs over Owens Valley observed by BAe-146 and King Air aircrafts during afternoon flights on 25 March.

Extensive studies have been conducted to use the radiosonde-measured temperature, the balloon rise rate, or estimated VV from the rise rate to characterize the wave activities in the atmosphere (e.g., Corby 1957; Reid 1972; Lalas and Einaudi 1980; Shutts et al. 1988; Allen and Vincent 1995). As shown in Fig. 9, the dominant features of the VV profiles in the stratosphere during T-REX are wavelike structures. In light of the horizontal drift of balloons, the question is whether these wavelike structures are caused by vertical or horizontal variations of the VV or a combination of two. In the example presented in Fig. 12, the balloon had drifted over ~150 km northeast by the time it reached the altitude of ~20 km. First, the magnitude of $\partial W_r/\partial z$ estimated from Fig. 12 is on an order of 3×10^{-3} s^{-1}. Based on the continuity equation, the change of horizontal wind velocity over 10 km horizontally should be 30 m s^{-1}, which is clearly impossible. Second, Gardner and Gardner (1993) concluded that if the horizontal winds are strong ($U/W_r > 10$), the distortion in balloon measurements of vertical wavenumber spectra could be significant. During T-REX, the horizontal winds were often 25–45 m s^{-1} in the stratosphere, implying a possible distortion. Third, the comparison of the VV from

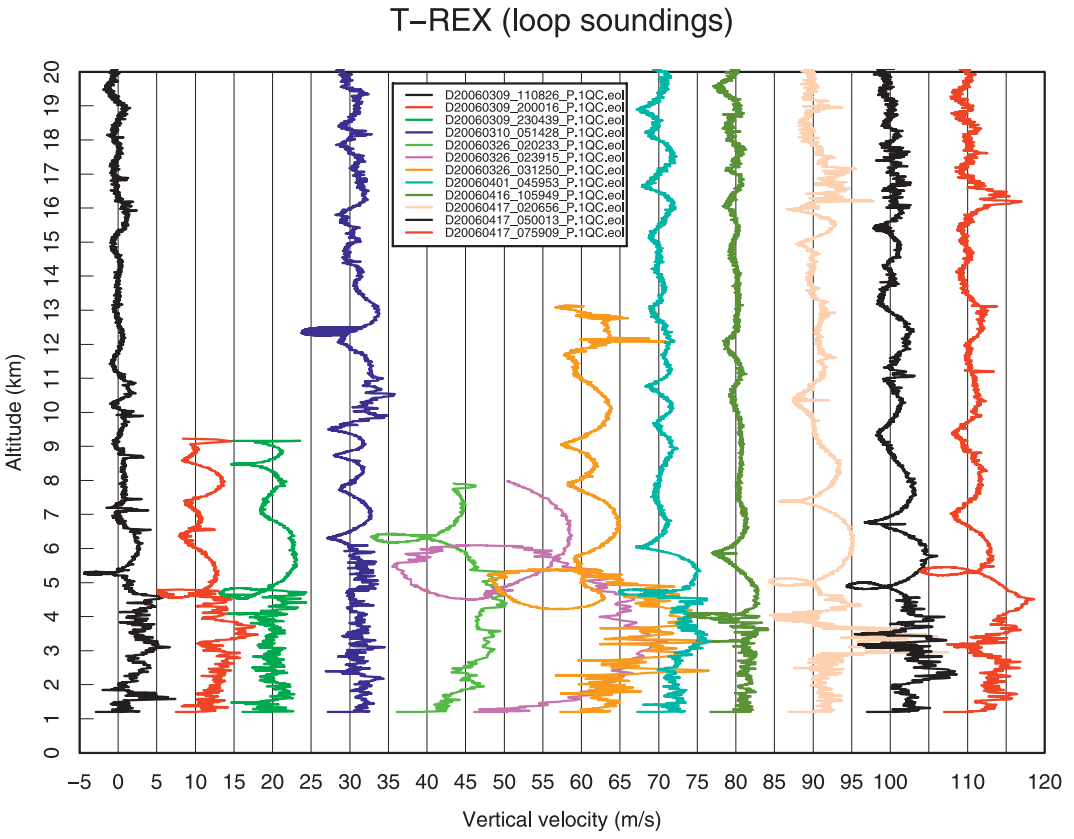

FIG. 10. Unfiltered VV profiles of 12 loop radiosonde soundings found during T-REX. A 10 m s^{-1} offset is added to each sounding after the first one. The VV of 110 m s^{-1} on the x axis means 0 m s^{-1} for the 12th sounding. The file names are given in the legend.

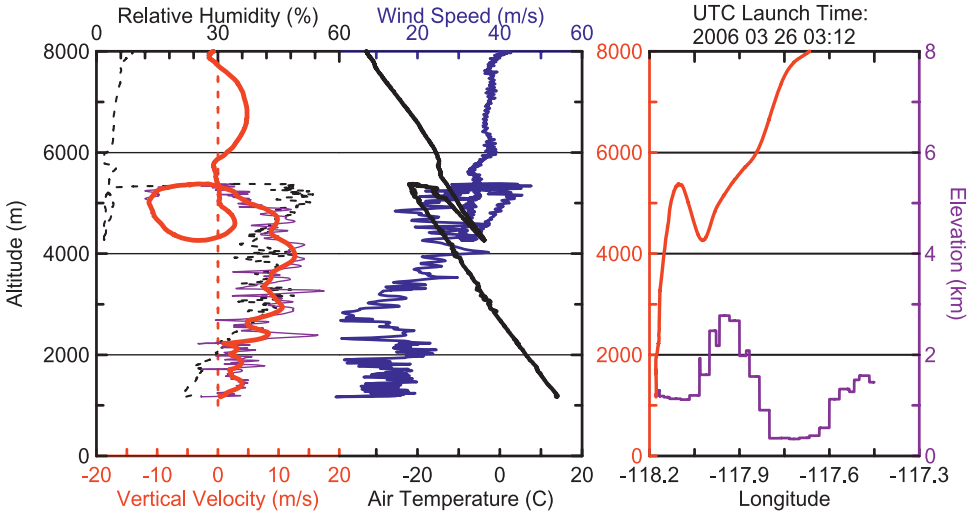

FIG. 11. (left) The unfiltered (thin solid purple) and filtered (thick solid red) VV, RH (dashed black), temperature (solid black), and wind speed (solid blue) profiles for the radiosonde launched at 0312 UTC 26 Mar 2006. (right) The balloon tracks on the longitude–altitude domain (red) and the terrain (purple).

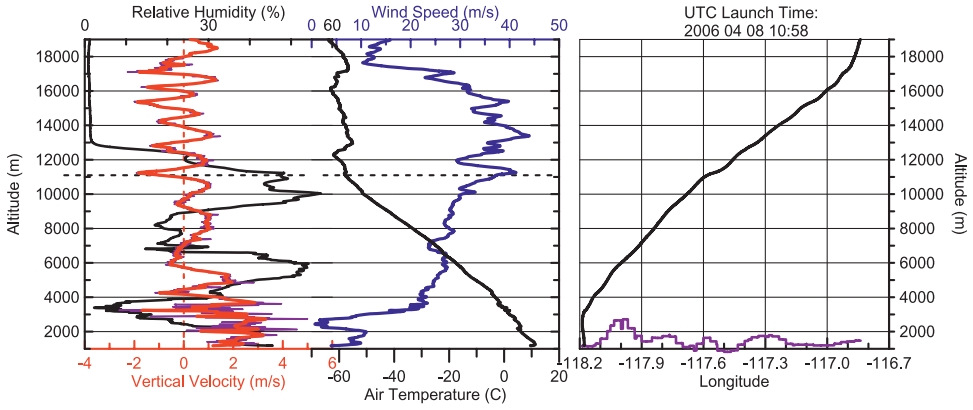

FIG. 12. (left) The unfiltered (thin solid purple) and filtered (thick solid red) VV, RH (solid black), temperature (solid black), and wind speed (solid blue) profiles for the radiosonde launched at 1058 UTC 8 Apr 2006. (right) The balloon tracks on the longitude–altitude domain (black) and the terrain (purple).

the radiosonde, dropsonde, and aircraft in Fig. 6 indicates that the VV profiles of radiosonde data represent horizontal variations of the VV. Fourth, Smith et al. (2008) show that the waves generated by the Sierra Nevada are primarily internal gravity waves by looking at the relations between energy and momentum fluxes. Therefore, we conclude that the wavelike structures represent mostly horizontal variations of the internal gravity waves and the vertical variation can be neglected. The horizontal wavelength of the waves is estimated by plotting the VV against the horizontal distance from the launch location. Figure 13 shows the histogram of the horizontal wavelength estimated from 75 identified waves. The wavelength ranges from 7 to 34 km with an average of ~15 km (Fig. 13). The magnitude of the estimated wavelength is comparable to that determined from the aircraft data (Smith et al. 2008). This exercise demonstrates the value of radiosonde-estimated VV in deriving the properties of waves in the stratosphere.

The last highlight is the 2D wind structure over Sierra Nevada and Owens Valley observed by the dropsondes along the southern leg during IOP 13 (see Fig. 4). A total of 30 dropsondes were deployed along the NCAR GV flight track over the Sierra Nevada and Owens Valley (Figs. 4, 14). For comparison, the wind data along the northern leg collected by the King Air at different altitudes are also exhibited in Fig. 14 (see Fig. 4). Strong waves are revealed in the dropsonde-estimated VV data, propagating perpendicularly to the mountain ridges and extending vertically from the ground to 8 km. They also have larger amplitudes in the lee side of Sierra Nevada with maximum peak-to-peak amplitude of ~24 m s^{-1} (Fig. 14). These waves were evident in the King Air measurements that were made ~55 km to the north, although the waves were weaker there. Smaller, more-detailed structures were uncovered by the dropsonde data because of the high vertical resolution of the dropsonde data. Figure 14 demonstrates how the estimated VV is valuable in mapping the detailed structure of vertical motions associated with waves, in addition to routine pressure, temperature, humidity, and horizontal wind profiles.

5. Conclusions and discussion

This study takes advantage of the high-quality, high-resolution radiosonde and dropsonde data and other aircraft and in situ data collected during T-REX to validate the sounding-estimated VV and demonstrate its value. The VV is the difference of the rise–fall rates between the actual and still atmosphere. The former is

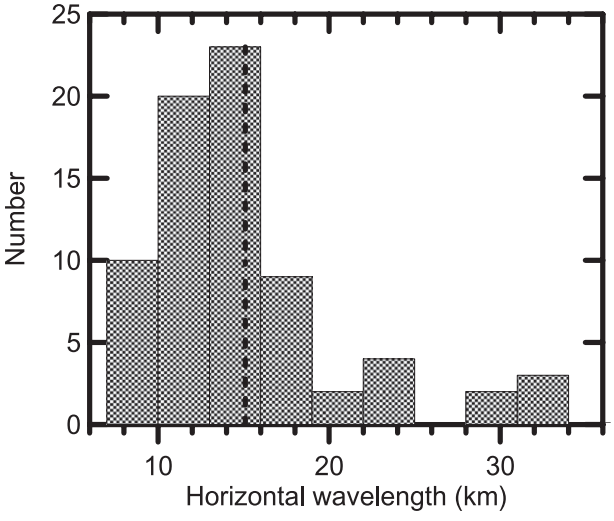

FIG. 13. The histogram of estimated horizontal wavelength of 75 waves. The vertical dashed line shows the mean (15.1 km).

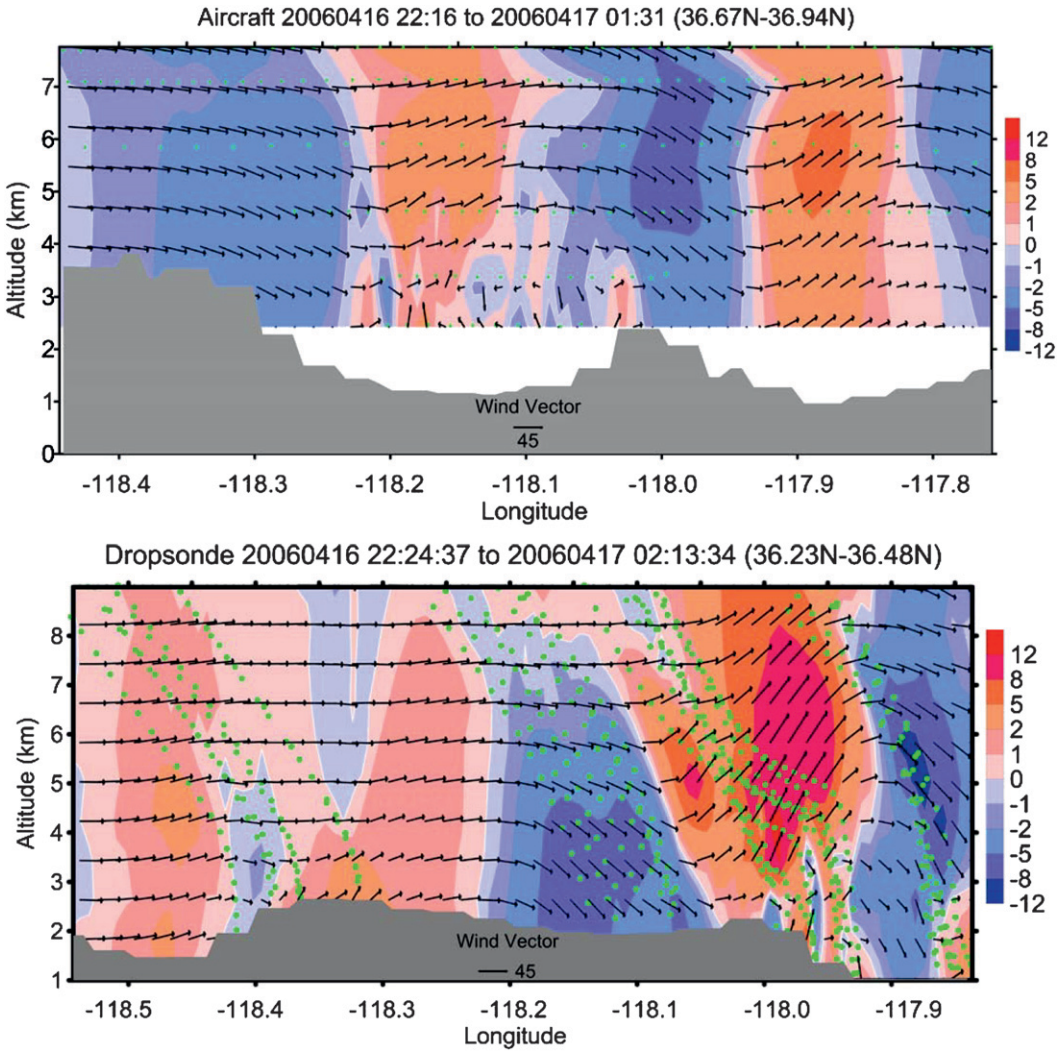

FIG. 14. (top) The longitudinal variations of VV profiles (color contour) from the King Air data along the northern leg during IOP 13 (see Fig. 4). Green dots are aircraft flight altitudes. (bottom) The longitudinal variations of VV profile (color contour) interpolated from the dropsonde data (green dots for dropsonde tracks) collected along the GV southern leg during IOP 13 (see Fig. 4). The wind vector represents zonal and vertical winds.

calculated from the time derivative of measured pressures, and the latter is computed based on the theory of the balloon motion in the still air. The methods for deriving the theoretical rise–fall rates are presented in detail and can be easily applied to other data. The techniques are applied to 102 GAUS radiosonde and 306 dropsonde soundings to create a T-REX sounding VV dataset for the T-REX community. The estimated VV is evaluated through comparisons among radiosonde, dropsonde, aircraft, and wind profiler data. The evaluation concludes that the vertical motion of the atmosphere can be estimated from the radiosonde (dropsonde) rise (fall) rate. The estimated VV is capable of capturing and describing the events with strong vertical motions ($>\sim$1 m s^{-1}) observed during T-REX. The dropsonde-estimated VV is more accurate than that from radiosonde. The radiosonde-estimated VV in the layers with strong turbulence has a positive bias because of uncertainty in the drag coefficient.

The VV profiles from the 102 radiosonde soundings show three distinct features: 1) strong vertical motions ($\sim$1–3 m s^{-1}) and large variability ($\sim$0.5–2.5 m s^{-1}) in the valley below the mountain ridge, 2) intensive downdrafts with magnitudes larger than the balloon rise rate resulted in descent of the balloons for a short period of time for 12 soundings, and 3) frequent occurrence of waves in the stratosphere. The radiosonde-observed waves are more representative of horizontal variations of gravity waves and have a mean horizontal wavelength of 15 km. The rapid and successive

deployment of dropsondes provides valuable data to depict detailed 2D structures of vertical and horizontal winds and thermodynamic parameters. The dropsonde-estimated VV clearly shows the strong mountain waves across the Sierra Nevada and Owens Valley. In conclusion, studying the sonde-estimated VV revealed several types of atmospheric phenomena associated with strong vertical motions and showed potential for more comprehensive studies of them and for other applications in the future.

There still remain some problems in estimating the VV using the sounding data, especially for radiosonde data. Based on this study, we make the following recommendations for more accurately deriving the VV from the sonde data. First, the high-resolution (preferably 1 s) radiosonde data should be recorded in all operational stations to accurately derive the rise–fall rates using the pressure tendency. Note that all current radiosonde archives only contain data at mandatory and significant pressure levels. The high-resolution radiosonde data are recorded for field or special projects, such as the U.S. high-resolution radiosonde dataset as part of the Stratospheric Processes and Their Role in Climate (SPARC) project for gravity wave studies (Allen and Vincent 1995). The U.S. National Weather Service started to archive the 1-s radiosonde data for stations using the new radiosonde ground system. Second, the GPS-measured rise–fall rates should be kept in the sonde data and are required for estimating the VV if the pressure-derived rise–fall rates are not available. Third, the balloon volume or the amount of helium put into the balloon before launch is an important parameter for computing the rise rate in the still air, but currently it is not measured accurately and not recorded at all. As a result, some assumptions have to be made to estimate the balloon volume (see section 2 for more details). Fourth, another uncertainty associated with the theoretical rise-rate calculation is the drag coefficient, especially under turbulent conditions. Some coincident, independent VV measurements can be made from wind profiler, lidar, or other techniques to help estimate the drag coefficient and understand its relationship with turbulence and other factors. Finally, the accuracy of the sonde-estimated VV is not quantified in this study resulting from a lack of large samplings of coincident, accurate, independent VV data. Special field campaigns should be designed for this purpose in the future.

Acknowledgments. The authors thank all participants in the T-REX field campaign for their contribution to the data collection effort. J. Bian is grateful to the NCAR EOL Science Group for supporting his 3-month visit to NCAR and is also supported by the National Natural Science Foundation of China under Grants 40675021 and 40775030. V.G.'s involvement in this study has been supported in part by the NCAR ASP Faculty Fellowship and NSF Grant ATM-0524891 to DRI. The T-REX data used in this study was obtained from the T-REX Data Archive, which was built and is maintained by NCAR EOL.

REFERENCES

Allen, S. J., and R. A. Vincent, 1995: Gravity wave activity in the lower atmosphere: Seasonal and latitudinal variations. *J. Geophys. Res.,* **100,** 1327–1350.

Balsley, B. B., W. L. Ecklund, D. A. Carter, A. C. Riddle, and K. S. Gage, 1988: Average vertical motions in the tropical atmosphere observed by a radar wind profiler on Pohnpei (7°N latitude, 157°E longitude). *J. Atmos. Sci.,* **45,** 396–405.

Contini, D., G. Mastrantonio, A. Viola, and S. Argentini, 2004: Mean vertical motions in the PBL measured by Doppler sodar: Accuracy, ambiguities, and possible improvements. *J. Atmos. Oceanic Technol.,* **21,** 1532–1544.

Corby, G. A., 1957: A preliminary study of atmospheric waves using radiosonde data. *Quart. J. Roy. Meteor. Soc.,* **83,** 49–60.

Franklin, J., M. L. Black, and K. Valde, 2003: GPS dropwindsonde wind profiles in hurricanes and their operational implications. *Wea. Forecasting,* **18,** 32–44.

Gage, K. S., J. R. McAfee, D. A. Carter, W. L. Ecklund, A. C. Riddle, G. C. Reid, and B. B. Balsley, 1991: Long-term mean vertical motion over the tropical Pacific: Wind-profiling Doppler radar measurements. *Science,* **254,** 1771–1773.

Gardner, C. S., and N. F. Gardner, 1993: Measurement distortion in aircraft, space shuttle, and balloon observations of atmospheric density and temperature perturbation spectra. *J. Geophys. Res.,* **98,** 1023–1033.

Grubišić, V., and Coauthors, 2008: The Terrain-induced Rotor experiment: A field campaign overview including observational highlights. *Bull. Amer. Meteor. Soc.,* **89,** 1513–1533.

Hock, T. F., and J. L. Franklin, 1999: The NCAR GPS dropwindsonde. *Bull. Amer. Meteor. Soc.,* **80,** 407–420.

Holton, J. R., 1992: *An Introduction to Dynamic Meteorology*. Academic Press, 507 pp.

Johansson, C., and H. Bergström, 2005: An auxiliary tool to determine the height of the boundary layer. *Bound.-Layer Meteor.,* **115,** 423–432.

Kim, Y.-J., S. D. Eckermann, and H.-Y. Chun, 2003: An overview of the past, present and future of gravity-wave drag parameterization for numerical climate and weather prediction models. *Atmos.–Ocean,* **41,** 65–98.

Lalas, D. P., and F. Einaudi, 1980: Tropospheric gravity waves: Their diction by and influence on rawinsonde balloon data. *Quart. J. Roy. Meteor. Soc.,* **106,** 855–864.

MacCready, P. B., Jr., 1965: Comparison of some balloon techniques. *J. Appl. Meteor.,* **4,** 504–508.

McHugh, J. P., I. Dors, G. Y. Jumper, J. R. Roadcap, E. A. Murphy, and D. C. Hahn, 2008: Large variations in balloon ascent rate over Hawaii. *J. Geophys. Res.,* **113,** D15123, doi:10.1029/2007JD009458.

Paluch, I. R., and D. H. Lenschow, 1991: Stratiform cloud formation in the marine boundary layer. *J. Atmos. Sci.,* **48,** 2141–2158.

Rao, T. N., K. N. Uma, D. N. Rao, and S. Fukao, 2008: Understanding the transportation process of tropospheric air entering the stratosphere from direct vertical air motion measurements

over Gadanki and Kotoabang. *Geophys. Res. Lett.,* **35,** L15805, doi:10.1029/2008GL034220.

Rauber, R. M., and A. Tokay, 1991: An explanation for the existence of supercooled water at the top of cold clouds. *J. Atmos. Sci.,* **48,** 1005–1023.

Reid, S. J., 1972: An observational study of lee waves using radiosonde data. *Tellus,* **6,** 593–596.

Shupe, M. D., P. Kollias, M. Poellot, and E. Eloranta, 2008: On deriving vertical air motions from cloud radar Doppler spectra. *J. Atmos. Oceanic Technol.,* **25,** 547–557.

Shutts, G. J., M. Kitchen, and P. H. Hoare, 1988: A large amplitude gravity wave in the lower stratosphere detected by radiosonde. *Quart. J. Roy. Meteor. Soc.,* **114,** 579–594.

Smith, R. B., B. K. Woods, J. Jensen, W. A. Cooper, J. D. Doyle, Q. Jiang, and V. Grubišić, 2008: Mountain waves entering the stratosphere. *J. Atmos. Sci.,* **65,** 2543–2562.

Stern, D. P., and S. D. Aberson, 2006: Extreme vertical winds measured by dropwindsondes in hurricanes. Preprints, *27th Conf. on Hurricanes and Tropical Meteorology*, Monterey, CA, Amer. Meteor. Soc., 16B.8. [Available online at http://ams.confex.com/ams/pdfpapers/108766.pdf.]

Vaisala, cited 2004: Vaisala RD93 GPS dropsonde. [Available online at http://www.vaisala.com/weather/products/soundingequipment/dropsonde.]

Van Zandt, T. E., 2000: A brief history of the development of wind-profiling or MST radars. *Ann. Geophys.,* **18,** 740–749.

Vennard, J. K., 1955: *Elementary Fluid Mechanics*. 7th ed. John Wiley & Sons, 401 pp.

Wang, J., 2005: Evaluation of performance of the dropsonde humidity sensor using data from DYCOMS-II and IHOP_2002. *J. Atmos. Oceanic Technol.,* **22,** 247–257.